Physical and Mechanical Properties of Polyethylene for Pipes in Relation to Molecular Architecture. II. Short-Term Creep of Isotropic and Drawn Materials

L. HUBERT,[1] L. DAVID,[1] R. SÉGUÉLA,[1] G. VIGIER,[1] C. CORFIAS-ZUCCALLI,[2] Y. GERMAIN[3]

[1] Groupe d'Etudes de Métallurgie Physique et de Physique des Matériaux, UMR CNRS 5510, INSA de Lyon, Bat. 502, 69621 Villeurbanne, France

[2] ATOFINA, Centre de Recherches et Développement, 27470 Serquigny, France

[3] ATOFINA, FINA Research, Zone Industrielle C, 7181 Feluy, Belgium

Received 8 May 2001; Accepted 10 September 2001

ABSTRACT: Tensile drawing and short-term creep of ethylene/α-olefin copolymers having bimodal (BM) molar weight distribution are studied in comparison with unimodal (UM) copolymers of similar crystallinity. The natural draw ratio and viscoelastic recovery upon unloading strongly suggest that BM copolymers have more tie chains and chain entanglements than corresponding UM copolymers. The incorporation of co-units in the longest chains of BM copolymers is ascribed a major role on these topological changes. Creep of isotropic materials shows lower compliance for BM copolymers in parallel with higher-durability grades. This is attributed to a better "macromolecular network efficiency." The creep behavior of strain-hardened samples, which is assumed to simulate the mechanical behavior of craze fibrils at the tip of a propagating crack, reveals similar trends. The better fibril strength in BM copolymers is again ascribed to a better network efficiency. Necked samples display an odd behavior of higher compliance at low stress and lower compliance at high stress for BM copolymers compared with the behavior of UM counterparts. This is associated with the exhaustion of viscoelastic capabilities with increasing draw ratio and stress. The phenomenon is discussed in relation to cavitation. A short-term creep test is proposed for comparative prediction of long-term behavior. © 2002 Wiley Periodicals, Inc. J Appl Polym Sci 84: 2308–2317, 2002

Key words: polyethylene; bimodal ethylene copolymer; tension test; creep; molecular structure

INTRODUCTION

The resistance to stress cracking of polyethylene and ethylene copolymers (PE) is the main requirement for applications in pipes for gas and water distribution. A number of studies have been carried out for the purpose of understanding the slow crack growth (SCG) phenomenon and improving the PE resistance to SCG through molecular architecture modifications (see, for instance, the introduction of the first study of this series).[1]

The most common way to assess the SCG resistance of materials for pipes is plotting the

Correspondence to: R. Séguéla (roland.seguela@insa-lyon.fr).
Contract grant sponsor: Conseil Régional Rhône-Alpes (France).

Journal of Applied Polymer Science, Vol. 84, 2308–2317 (2002)

stress versus time-to-failure diagram at various temperatures, using either pieces of pipes under pressure or notched cylindrical or parallelepipedic samples in tensile tests. Such diagrams usually display two failure regimes.[2–5] At high stress levels and short times, ductile failure is associated with the plastic yielding of the material. The plastic instability phenomenon, characteristic of high-density PE, is responsible for the occurrence of localized plastic deformation, which takes the form of a parrot-beak protrusion, parallel to the main axis in the case of pipes.[6] The necked material then fails by a transverse crack. At low stress levels and long times, brittle failure of pipes occurs as a crack propagating through the pipe wall, parallel to the main axis.[6] PE brittle failure has been claimed by a number of investigators to originate from chain disentanglement, seemingly by analogy with the crazing process of glassy polymers close to the glass-transition temperature. Chain rupture may also be a likely mechanism, given that it has often been assumed for modeling the rupture of fibers of semicrystalline polymers, including PE. In the SCG process, the breaking of intercrystalline tie chains might be involved either in the fibrils formed at the tip of a propagating crack or in the amorphous layers of the isotropic material, at the stage of crack initiation. This point was previously addressed in the introductory section of the former study.[1]

The ductile–brittle transition revealed by the stress versus time-to-failure plot is a major feature for PE pipe applications. Indeed, time to failure increases faster with decreasing stress in the ductile domain than in the brittle domain. Thus, the location of the ductile–brittle transition determines the lifetime in service of a given material. This transition is strongly dependent on the molecular structure and morphology of PE. The higher the crystallinity, the longer the time for ductile failure, at a given stress level. However, this is generally accompanied with an early occurrence of the brittle regime. In contrast, high molecular weight chains as well as short chain branches (SCBs) incorporated by copolymerization of α-olefin co-units can lead to a significant shift of the brittle regime to long failure times. Unfortunately, a concomitant downward shift of the stress versus time curve in the ductile domain occurs in the case of copolymers, attributed to reduced crystallinity compared to that of homopolymers; moreover, high molecular weight PE exhibits drastically reduced processing ability.

Developments in polymerization processes in recent years have opened routes to novel copolymers having bimodal molar weight distributions (MWD) and co-units preferentially located in the high MW population. Such materials display a substantial shift of the ductile–brittle transition to both longer time and higher stress, compared with that of conventional PE issued from either Ziegler–Natta (ZN) or chromium oxide (CrO_2) catalysis, at equivalent crystallinity.[7] Preferred incorporation of co-units in the long chains has been claimed by several authors to be a route for improving long-term behavior,[7–13] although the precise origin of this phenomenon is not yet well understood.

In the first study of this series,[1] we reported a detailed analysis of the molecular architecture of bimodal ZN and unimodal CrO_2 copolymers. Besides a clear-cut bimodal MWD, the bimodal copolymer displayed a modification of the co-unit distribution with respect to unimodal copolymers, that is, a preferred location of the co-units on long chains. Although such modification might seem unimportant at first sight, it proved to have a drastic effect on the long-term properties. We discussed this effect as an increase of chain entanglement and tie chain densities resulting from reduced propensity of long chains with SCB to regular chain folding and chain reeling during crystallization.

The duration of the complete stress versus time evaluation of any new PE material for tube application is so long that any kind of short-term test leading to a qualitative predictive assessment of long-term properties should prove to be of great value. Thus, the investigation of physical parameters on which durability is suspected to depend has been proposed to get comparative evaluation of materials having well-characterized lifetimes. Crystallization kinetics that are known to influence the molecular topology of the solid materials, notably regarding intercrystalline tie chains and chain entanglements, were investigated in the first study of the series.[1] It was suspected that slow kinetics roughly correlate with high durability as a result of more numerous interlamellar connections. It turned out that the molecular architecture modification of bimodal copolymers compared with unimodal ZN copolymers affects crystallization kinetics to such an extent that there is no longer a correlation with durability.

It has also been proposed by some investigators that the fibrillar structure of PE stretched to its natural draw ratio could be taken as a model for

Table I Molecular and Physical Characteristics of the Copolymers

Copolymer	Co-unit MWD[a]	Methyl (CH_3‰C)	M_n (kg/mol)	M_w (kg/mol)	M_z (kg/mol)	Density (g/cm^3)	X_c[b] (w %)	Durability Grade
CP1	Hexene/UM	4.3	9.3	183	1470	0.940	57	PE80
CP2	Hexene/UM	1.6	11.7	207	1530	0.946	63	PE80[c]
CP3	Hexene/BM	2.4	11.8	220	1540	0.948	65	PE100
CP4	Butene/UM	2.4	9.1	236	1580	0.945	67	PE63
CP5	Butene/BM	3.5	10.2	215	1160	0.944	66	PE80

[a] MWD, molar weight distribution; UM, unimodal; BM, bimodal.
[b] Crystallinity assessed from differential scanning calorimetry (Hubert et al., 2001).
[c] CP2 is a PE80 grade for tube applications but is not far from the PE100 standard.

studying the mechanical behavior of the microfibrils at the tip of a propagating crack. Capaccio and coworkers[14,15] have indeed shown a quite amazing correlation between the creep resistance of such drawn materials with the stress cracking resistance of the isotropic materials, over a wide range of crystallinity. In another connection, Laragon et al.[16] have shown from a Raman spectroscopy study on a series of high-density PE drawn to their natural draw ratio that, for a given macroscopic strain, the higher the stress cracking resistance, the less stressed are the mechanically active chains.

The present work deals with a mechanical study of isotropic and drawn copolymers by creep experiments, to establish correlations with molecular architecture and chain topology. Indeed, if resistance to creep is ascribed to the strength of the physical network made of stiff crystalline lamellae bound by intercrystalline tie molecules and entangled chain loops, such tests would provide direct indication of the physical network efficiency. A second goal of the study is to put forward a short time test that would be able to provide qualitative assessment of the long-term behavior of any PE material by comparison with previously characterized materials.

EXPERIMENTAL

The chemical and physical characterizations of the five ethylene copolymers investigated in this work were previously described in the former study.[1] Table I reports the main characteristics of these materials. Melt-cast 1-mm-thick sheets were prepared by compression-molding at 160°C for 5 min, and cooled at about 20°C/min.

Drawing was carried out on a model 1/ME MTS tensile-testing machine (MTS Systems Corp., France) equipped with an air-pulsed oven and pneumatic grips. The H2-type dumbbell-shape samples (20 and 5 mm in gauge length and width, respectively) were cut out from the sheets with a punching die. Two types of drawn specimens were prepared at the draw temperatures (T_d's) of 20 and 80°C, at a crosshead speed of 50 mm/min. The first type consisted of drawing beyond the yield point and propagating the neck over a 60-mm length. The so-called natural draw ratio[17] λ_n was determined from the reduction of cross section in the necked region. Measurements were carried out on both stressed samples, prior to unloading, and on unloaded samples after 24-h relaxation at 20°C. This allowed an assessment of the recovery ability of the drawn materials. The second type of specimen consisted of drawing the material in the strain-hardening domain, in the midrange between λ_n and the breaking strain. The actual draw ratio was about 80% of the breaking strain at 20°C and 60% at 80°C. This was called the *strain-hardened* state.

Creep experiments were performed on an MTS machine (model 1/ME) at constant force, on both isotropic and drawn copolymers, at 20 and 80°C. The parallelepipedic specimens were cut from either the isotropic compression-molded sheets ($\sim 30 \times 4 \times 1$ mm), the necked samples ($\sim 30 \times 2 \times 0.6$ mm), or the strain-hardened samples ($\sim 30 \times 1.5 \times 0.4$ mm). For the two types of drawn materials, the specimens were allowed to relax unloaded for 72 h before creep testing, to achieve full viscoelastic recovery. For all creep tests, the initial sample loading was conducted at a crosshead speed of 50 mm/min, so that the force level for every experiment was reached within less than 15 s without stress overshoot. The compli-

Table II Physical Parameters of the Drawn Copolymers

Copolymer	λ_n at 20°C[a]	Recovery at 20°C[b] (%)	λ_{max} at 20°C	λ_n at 80°C[a]	λ_{max} at 80°C
CP1	5.3 ± 0.1	10 ± 1%	11.0 ± 0.3	4.8 ± 0.1	14.0 ± 0.3
CP2	5.7 ± 0.1	11 ± 1%	10.5 ± 0.3	4.9 ± 0.1	15.5 ± 0.3
CP3	5.1 ± 0.1	13 ± 1%	10.5 ± 0.3	4.5 ± 0.1	15.5 ± 0.3
CP4	6.8 ± 0.1	12 ± 1%	9.5 ± 0.3	5.7 ± 0.1	17.0 ± 0.3
CP5	5.4 ± 0.1	15 ± 1%	9.0 ± 0.3	4.9 ± 0.1	14.0 ± 0.3

[a] Measured unloaded.
[b] Recovery = [λ_n (constrained) − λ_n (unloaded)]/λ_n (constrained).

ance was computed from the ratio of the strain to the stress. Assuming uniform deformation, the change of sample length between the grips was taken into consideration for the strain measurement and the sample cross section prior to loading was used for computing the stress. All the creep compliance data reported in this study were determined at a creep time of 15 min, that is, in the secondary creep domain where compliance is less sensitive to time for all the stress range investigated. It is worth noticing that unreported compliance data at 45 min creep showed similar trends as a function of stress. In contrast, compliance data at 5 min creep (i.e., in the primary creep domain) displayed significantly larger uncertainty than 15-min data and did not allow relevant comparisons of the various materials.

Throughout all phases of the creep behavior study, the lower limit of the stress scale of the compliance versus stress plots was the upper limit of linear viscoelastic behavior, that is, the lower stress for which compliance is no longer independent of stress. The upper limit of the stress in the case of isotropic samples is the one for which necking does not occur during the 15-min creep test. In the case of drawn samples, the limiting stress is that for which samples are pulled out of the grips or break within the test time.

RESULTS AND DISCUSSION

Uniaxial Drawing

Table II displays some physical parameters of the copolymers drawn either to necking or to rupture. At both T_d values of 20 and 80°C, the natural draw ratio as measured in the stable neck is systematically smaller for the bimodal copolymers than that for the unimodal copolymers of equivalent crystallinity and co-unit type, that is, CP3 versus CP2 and CP5 versus CP4. In a primary approach of macromolecular network stretching, the natural draw ratio λ_n may be related to the concentration of chain segments between entanglements ν through the following relation[18–20]:

$$\lambda_n = C/\sqrt{\nu}$$

where the constant C depends only on the polymer nature. In this instance, the above finding can be taken as a piece of evidence that the entanglement density of bimodal copolymers is somewhat higher than that of corresponding unimodal copolymers. Table II also displays pertinent data regarding the relaxation behavior upon unloading of the necked samples at T_d = 20°C: bimodal CP3 and CP5 copolymers exhibit higher viscoelastic strain recovery than that of unimodal CP2 and CP4 copolymers, respectively. Unreported data at T_d = 80°C do not allow relevant comparison because of the large relative uncertainty on the recovery capacity. Nonetheless, the recovery data for T_d = 20°C give indication of a greater network strength for bimodal copolymers that is thoroughly consistent with the above-noted conclusion of a greater entanglement density.

Creep of Isotropic Samples

Typical compliance versus time plots are reported in Figure 1 in the case of isotropic CP2 copolymer at 20°C. After the instantaneous elastic loading, compliance increases rapidly with increasing time in the primary creep domain. This increase of the compliance gradually slows down as secondary creep takes place with a constant rate. Below the stress level of 8 MPa, the almost identical creep curves (not shown in Fig. 1) are indic-

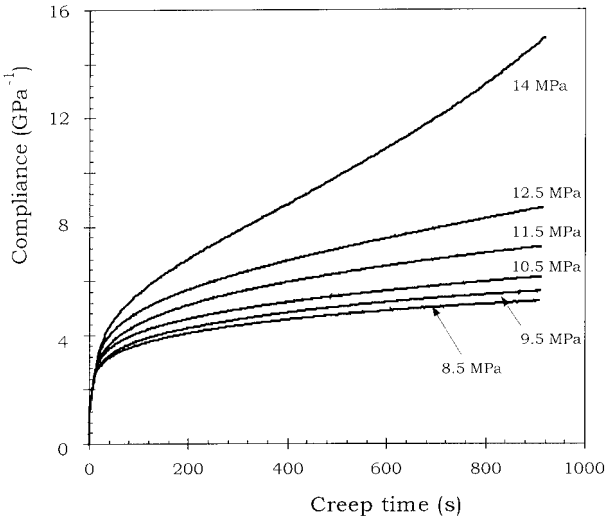

Figure 1 Creep curves of isotropic copolymer CP1 for various stress at 20°C.

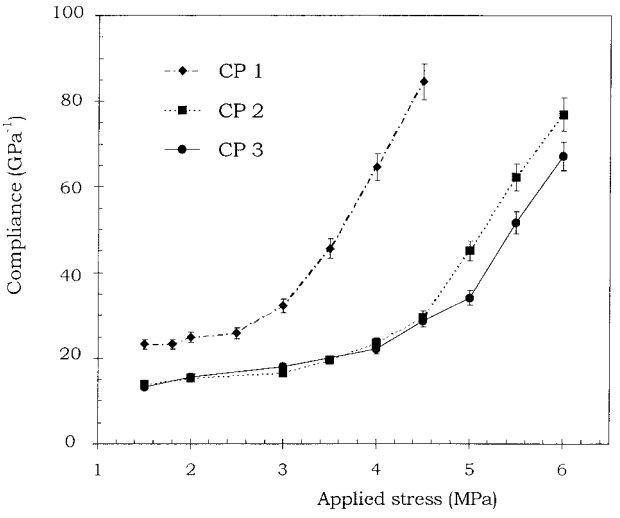

Figure 3 Compliance versus stress plots at 80°C of isotropic copolymers CP1, CP2, and CP3.

ative of a linear viscoelastic behavior. Above 8 MPa, compliance turns out to be sensitive to stress: the higher the stress level, the greater the departure from the linear behavior. For an applied stress of 14 MPa, the acceleration of the compliance increase between 600 and 900 s is relevant to the ternary creep regime (Fig. 1). For applied stresses above 18 MPa, plastic instability takes place within the 15 min of the creep tests, accompanied with a drastic upswing of the compliance. Similar observations were made for the other copolymers under investigation.

Figures 2 and 3 show the compliance versus stress plots for the CP1, CP2, and CP3 copolymers in the isotropic state, at 20 and 80°C, respectively. For both temperatures, CP1 displays a greater compliance over the whole stress range than that of the two other copolymers. This observation is consistent with its significantly lower durability grade, in conjunction with a slightly lower crystallinity. CP2 is more compliant than CP3, but not significantly so. This is in line with the fact that CP2 does not reach the PE100 grade but almost achieves this classification (see Table I).

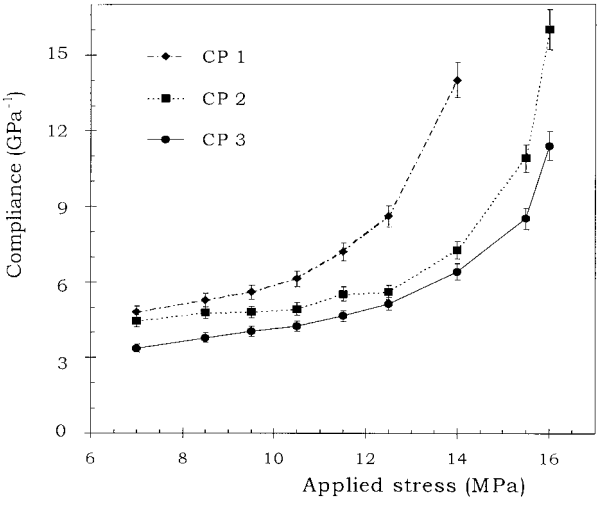

Figure 2 Compliance versus stress plots at 20°C of isotropic copolymers CP1, CP2, and CP3.

Figures 2 and 3 clearly exhibit a compliance hierarchy of the three copolymers that matches the durability ranking of Table I. The density of intercrystalline tie molecules is suspected to be the connection between the two kinds of mechanical evaluations. Indeed, tie chains that ensure the mechanical link between the crystallites, through the rubbery amorphous layers in semicrystalline polymers, constitute the weaker point of the stress transfer process resulting from their relatively low frequency in ethylene-based polymers having a high propensity for chain-folding crystallization. Thus, tie chains should be one of the main parameters controlling both short-term creep and long-term behavior, at a given crystallinity level. As a matter of fact, the bimodal CP3 copolymer that was shown in the former study[1] to contain more tie chains and chain entanglements than those of CP2 (attributed to hindrance of molecular architecture complexity on crystallization kinetics) is less compliant and more stress crack resistant than CP2. Short-term creep thus

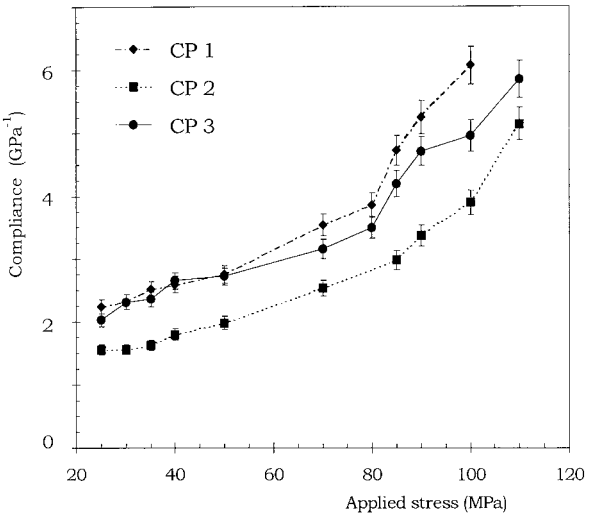

Figure 4 Compliance versus stress plots at 20°C of copolymers CP1, CP2, and CP3 neck-drawn at 20°C.

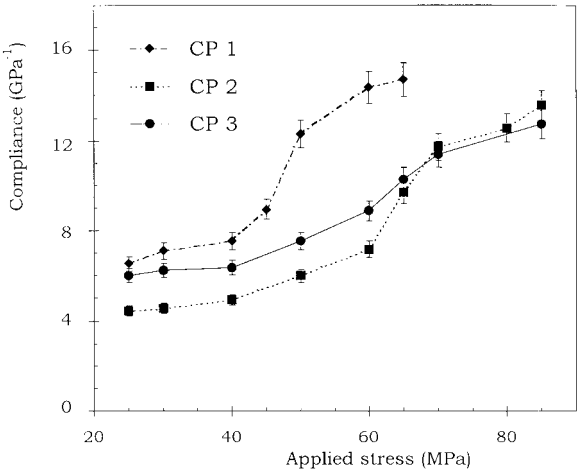

Figure 6 Compliance versus stress plots at 80°C of copolymers CP1, CP2, and CP3 neck-drawn at 20°C.

appears as a relevant means to anticipate long-term properties of PE materials.

Creep of Neck-Drawn Samples

Samples drawn to the stage of natural draw ratio have a fibrillar structure that is assumed to be analogous to that of the craze fibrils that form at the tip of a propagating crack in the stress domain of brittle failure. Such drawn samples have been tested in creep to simulate the mechanical behavior of the damaged zone at a crack tip.

Figures 4 and 5 show the compliance versus stress for creep tests conducted at 20°C on copolymers CP1, CP2, and CP3 drawn at T_d values of 20 and 80°C, respectively. Of the three, CP1 is the most compliant copolymer over the whole stress range. This is quite logical with regard to the slightly lower crystallinity and is consistent with long-term behavior. However, the higher compliance of CP3 versus CP2, for both cases of drawing at 20 and 80°C, is quite surprising. This does not support the copolymer ranking in durability (Table I).

Figures 6 and 7 report the creep compliance at 80°C versus stress for the same copolymers drawn at 20 and 80°C, respectively. In this instance, CP3 copolymer exhibits higher compliance than CP2 over only a part of the stress

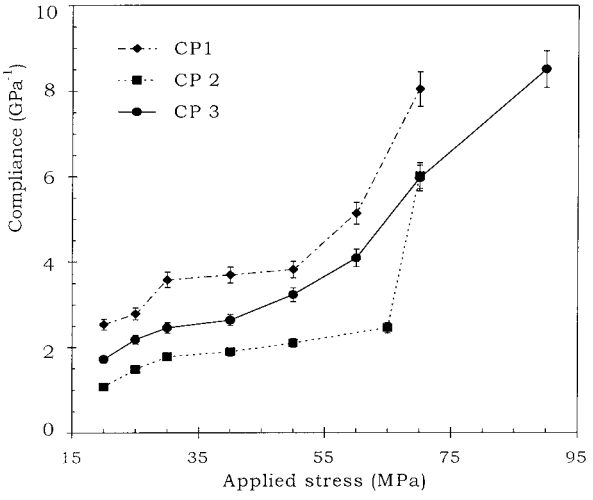

Figure 5 Compliance versus stress plots at 20°C of copolymers CP1, CP2, and CP3 neck-drawn at 80°C.

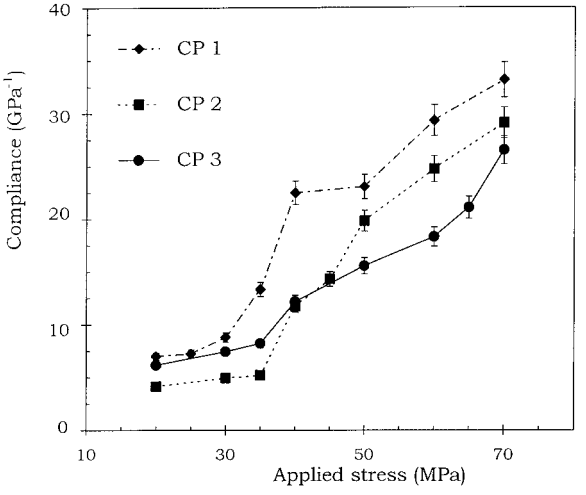

Figure 7 Compliance versus stress plots at 80°C of copolymers CP1, CP2, and CP3 neck-drawn at 80°C.

range, that is, lower stresses. The slope of the compliance versus stress curve of CP3 is indeed weaker than that of CP2, so that the two curves cross themselves at about the midstress range.

These findings are quite puzzling with regard to the preceding conclusions on the creep behavior of isotropic materials, and also to the copolymer ranking in durability. An explanation can be devised from the characteristics of the drawn samples (Table II) (already discussed in the subsection, Uniaxial Drawing). The higher recovery of bimodal copolymers upon unloading from the necked state is relevant to a stronger viscoelastic strain component that confers greater compliance to CP3, compared with that of unimodal parent CP2, notably at low stress. However, the viscoelastic capacities of PE are well known to be gradually exhausted as strain increases in the strain-hardening range.[21,22] This effect is all the more pronounced when the draw temperature is high because of the improved degree of crystalline organization and crystal block size in the fibrillar structure. A consequence is that, as the applied stress increases in the creep tests, the viscoelastic component of the necked samples is gradually reduced and the Langevin-like response[23] of the stretched macromolecular network exerts an increasing contribution. This does not seem to be able to reverse the compliance versus stress trend for the 20°C creep (Figs. 4 and 5). However, for creep at 80°C (Figs. 6 and 7), it appears that the viscoelastic response of necked CP3 turns out readily exhausted for the higher stresses of the experimental stress range, so that CP3 becomes less compliant than CP2 at high stress. It is worth noticing that this process takes place faster for a draw temperature of 80°C (Fig. 7) than that at 20°C (Fig. 6) because of lesser viscoelastic capacities of the fibrillar structure buildup at high temperature.

Combined effects of different viscoelastic capacities and different physical network properties result in a rather complex creep behavior of the neck-drawn copolymers. No clear-cut correlation appears between short-term creep of such neck-drawn samples and long-term behavior of isotropic copolymers, so this approach does not seem adequate for discriminating PE materials for pipe applications.

Creep on Strain-Hardened Samples

Samples drawn in the strain-hardening range were tested in creep, as for simulating the mechanical behavior of the craze fibrils close to rupture in a propagating crack. The compliance versus stress data for copolymers CP1, CP2, and CP3 are reported in Figure 8 for drawing and creep at 20°C. CP1 is slightly more compliant than either CP2 or CP3 at low stress. Then, CP3 gradually departs from CP2 and CP1 by retaining a lower compliance as stress increases. It seems that the viscoelastic effect responsible for the rather complex creep behavior of the neck-drawn sample is significantly reduced in the present case of strain-hardened samples. This is consistent with the exhaustion of the viscoelastic capabilities of drawn PE when the plastic strain is increased in the strain-hardening domain, as discussed above. The network contribution to the compliance is thus improved as viscoelasticity is exhausted.

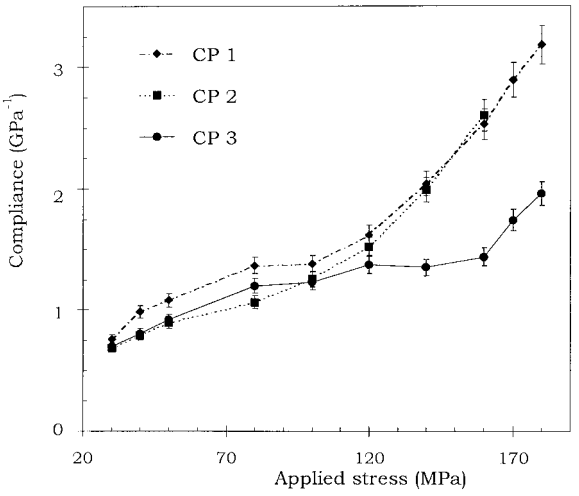

Figure 8 Compliance versus stress plots at 20°C of copolymers CP1, CP2, and CP3 strain-hardened at 20°C.

Figure 9 shows the data for drawing and creep at 80°C. CP1 is much more compliant than the two other copolymers over the whole stress range. CP2 is also more compliant than CP3, although the departure is more pronounced at high stress. It seems that the viscoelasticity exhaustion is still more important when strain-hardening is carried out at 80°C compared with that at 20°C. As suggested in the previous subsection, this can be assigned to an improvement of crystalline organization in the fibrillar structure.

Additional data for CP4 and CP5 are also reported in Figure 9. CP4 clearly exhibits a higher compliance level over the whole stress range together with a significantly lower value of the stress limit that can be applied without rupture

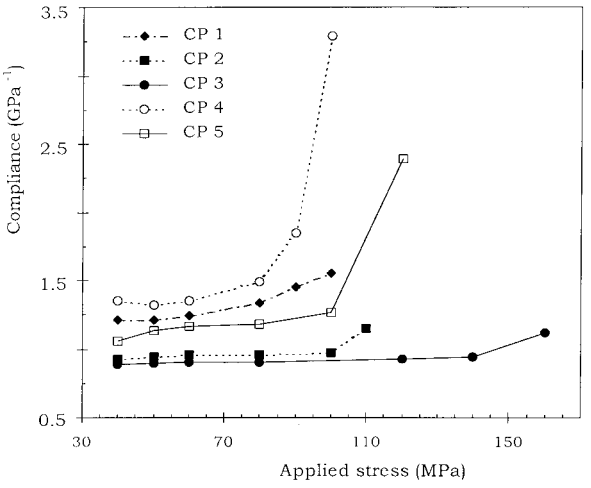

Figure 9 Compliance versus stress plots at 80°C of the five copolymers strain-hardened at 80°C.

during the 15-min creep test. This is perfectly consistent with the PE63 grade of this copolymer. The bimodal CP5 is closely related to CP2, given that both copolymers are of PE80 grade; nevertheless, the upper stress limit is higher for CP5.

For both temperatures, the strain-hardened samples of CP3 no longer display the complex behavior of the necked samples (Figs. 6 and 7), that is, a higher compliance than CP2 at low stress, which turns lower at high stress. This can be readily ascribed to the exhaustion of the viscoelastic capacities as plastic strain grows in the strain-hardening domain, which makes the macromolecular network efficiency become predominant on the compliance. This effect is more pronounced for drawn samples at 80°C because of improved crystalline organization.

The creep behavior of strain-hardened samples at 80°C proves to be a fairly discriminating test for copolymers of close crystallinity levels but various durability grades, irrespective of the molecular architecture. It is likely to be a relevant method for short-term evaluation of materials intended for pipe applications.

CONCLUSIONS

The analysis of natural draw ratio and strain recovery capacity upon unloading provides evidence of greater chain entanglement and tie chain densities for bimodal copolymers compared with those of their unimodal counterparts. Considering that SCB from co-units and high molecular weight chains have a similar capacity to involve a high rate of chain entanglements and intercrystalline tie chains, the preferred incorporation of SCB on long chains in bimodal copolymers has been attributed by several investigators to be highly beneficial for chain topology (see the previous study[1] and references cited therein). However, we suggest in addition that the very origin of the increasing densities of tie chains and chain entanglements lies in the better efficiency of such co-unit–rich long chains for disrupting the mechanisms of regular chain folding and chain disentanglement during crystallization. This interpretation is in agreement with the conclusions from the former study[1] of the series regarding the physical properties and crystallization kinetics of the present copolymers.

Short-term creep on isotropic samples reveals a similar trend of better molecular network efficiency of bimodal copolymers but is less discriminating than natural draw ratio and strain recovery. This is ascribed to the fact that, in both approaches, the physical network of crystalline lamellae (creep of isotropic materials) or microfibrils (drawn materials), bound by tie chains and entangled chain loops, is the main factor of mechanical strength. In contrast to isotropic samples, necked samples display a complex creep behavior as a function of stress level, resulting from a stronger viscoelastic strain component of bimodal copolymers compared with that of unimodal copolymers, at low stress. Drawing in the strain-hardening range improves the macromolecular network contribution because of the viscoelasticity exhaustion, notably for high draw temperature. Creep of strain-hardened samples turned out to be a discriminating test. It is worth mentioning that, for the sake of validation of this test, a collection of 15 commercial copolymers of PE80 and PE100 grades were tested and successfully classified with regard to their stress versus time to rupture behavior.

It is obvious that the so-called macromolecular network is not the same for the isotropic state with lamellar structure and for the drawn state with fibrillar structure. However, direct filiation exists by means of chain-unfolding processes that turn a number of chain folds of the lamellar structure into intercrystalline tie chains in the fibrillar structure. Original tie chains and chain entanglements that govern the drawability of the material should be essentially preserved throughout plastic drawing. This is borrowed from Peterlin's model[24] for the fibrillar transformation that has

often been modified or amended but never denied. The radical change of long period in the fibrillar structure, compared with that in the mother lamellar structure, has been claimed by some investigators to be an evidence of some kind of melting–recrystallization process. However, it is clear that some of the topological features of the macromolecular network are well preserved. The fact that the creep displays similar trends for isotropic and strain-hardened samples and leads to the same copolymer ranking supports the idea that the macromolecular networks are closely related in the two cases. This means that all architectural and topological features contributing to the mechanical strength of the fibrils at the tip of a propagating crack are also likely to improve the material strength at the early stage of crack initiation in the original lamellar structure. The probability for breakage of tie chains under static stress, as well as chain disentanglement if any, will decrease as the density of tie chain and chain entanglement increases, given the reduced force acting on any of these elements.

Although this study refers only to experiments involving plastic properties on a short-term scale, the conclusions on the strength of the macromolecular network in terms of resistance to chain rupture and/or chain disentanglement provide a substantial body of data to understand the long-term properties, both in the ductile regime where failure occurs by interfibrillar separation after plastic yielding and in the brittle regime where failure proceeds by SCG. Indeed, besides the crystallinity level, which governs the plastic flow stress in the ductile regime, the entanglement density of the chain network determines the capacity of resistance to plastic instability (high natural draw ratio and low strain-hardening). In the brittle regime, the breaking stress of the fibrils pulled out from the lips of the opening crack is governed by the strength of the more or less extended chain network, that is, the chain entanglement and tie chain densities. We suggest that all parameters of the molecular architecture that are likely to increase the entanglement density will improve the long-term behavior. This has been already claimed by Brown and coworkers regarding SCG (see the discussion in the first study[1] of this series). However, crystallinity must not decrease in parallel, given that it is a detrimental factor for the stress level in the ductile regime. This is precisely the challenge that has been achieved through the synthesis of bimodal copolymers.

The question remains on the origin of the higher viscoelastic recovery of neck-drawn bimodal copolymers, compared with unimodal copolymers at equivalent crystallinity, that has notably been assigned a determining role in the complex creep behavior of neck-drawn CP3. It is worth mentioning that no viscoelasticity effect has been suggested to contribute to the compliance of isotropic copolymers. Thus, it is suspected that the origin of the pronounced viscoelasticity neck-drawn CP3 arises from some peculiar strain-induced phenomenon during plastic deformation. In this instance, first hints of interpretation can be proposed from a small-angle X-ray scattering study in progress that revealed stronger interfibrillar cavitation in neck-drawn bimodal copolymers, compared with that in unimodal copolymers at equivalent crystallinity. The opening upon loading of interfibrillar microvoids and the closing of these microvoids upon unloading stemming from the entropic back-stress of the rubbery amorphous chains is likely to bring about a viscoelastic effect. The origin of the higher cavitation propensity of bimodal copolymers may be ascribed to their specific molecular architecture. Indeed, in spite of the fact that the longest chains in both bimodal and unimodal copolymers are thoroughly deprived from co-units, bimodal copolymers have the co-units concentrated on longer chains than their unimodal parents, as shown in the first study of this series.[1]

Thus, bimodal copolymers can be regarded, in first approximation, as two interpenetrating macromolecular networks made of co-unit–rich long chains and almost linear chains of both medium and short length. The latter chain population is highly detrimental for the molecular cohesion of the material because of the well-known effect that short chains and SCB deficiency both reduce the ability of PE to build up intercrystalline tie chains during crystallization. Besides, evidence of phase separation of the various chain species in the midtemperature range of crystallization of bimodal copolymers is also likely to reduce the tie chain frequency.[1] This is suspected to give rise to highly compliant and cavitation-prone zones. However, it turns out that the network strength gained from the co-unit–rich long chains largely compensates this deficiency. It substantially improves the short-term creep resistance and long-term behavior of the bimodal copolymers. In addition, it may be ascribed a major part in the viscoelastic recovery upon unloading of the vol-

ume strain accompanying the microvoid opening under stress.

In summary, given the analogy of the chain topology in the isotropic state and the strain-hardened state, both short-term creep of drawn samples and long-term behavior of extruded tubes have been correlated with the molecular architecture of the copolymers. From a practical standpoint, this study provides a very useful means for evaluating long-term properties of copolymers from short-term creep tests.

The Conseil Régional Rhône-Alpes is deeply acknowledged for the grant of a doctoral fellowship to L. Hubert.

REFERENCES

1. Hubert, L.; David, L.; Séguéla, R.; Vigier, G.; Degoulet, C.; Germain, Y. Polymer 2001, 42, 8425.
2. Lustiger, A.; Markham, R. L. Polymer 1983, 24, 1647.
3. Choi, S.; Broutman, L. J. in Proceedings of the 44th ANTEC Conference of the Society of Plastic Engineers, Boston, MA, April 1986; pp 592–599.
4. Kausch, H.-H. Polymer Fracture; Springer Verlag: Berlin, 1987; Chapter 1.
5. Gedde, U. W.; Viebke, J.; Leijström, H.; Ifwarson, M. Polym Eng Sci 1994, 34, 1773.
6. Ben Hadj Hamouda, H.; Simoes-Betbeder, M.; Grillo, F.; Blouet, P.; Billon, N.; Piques, R. Polymer 2001, 42, 5425.
7. Berthold, J.; Böhm, L. L.; Enderle, H.-F.; Göbel, P.; Lüker, H.; Lecht, R.; Schulte, U. Plast Rubber Compos Process Appl 1996, 25, 368.
8. Ishikawa, N.; Shimizu, T.; Shimamura, Y.; Goto, Y.; Omori, K.; Misaka, N. in Proceedings of the 10th Plastic Fuel Gas Pipe Symposium of the American Gas Association, New Orleans, LA, 1987; pp 175–183.
9. Lustiger, A.; Ishikawa, N. J Polym Sci Part B: Polym Phys 1991, 29, 1047.
10. Scholten, F. L.; Rijpkema, H. J. M. in Proceedings of the Plastics Pipes Conference VIII of The Plastics and Rubber Institute, Koningshof, The Netherlands, September 1992, C2/4; pp 1–10.
11. Brown, N.; Lu, X.; Huang, Y.; Harrison, I. P.; Ishikawa, N. Plast Rubber Compos Process Appl 1992, 17, 255.
12. Saeda, S.; Suzaka, Y. Polym Adv Technol 1995, 6, 593.
13. Clutton, E. Q.; Rose, L. J.; Capaccio, G. Plast Rubber Compos Process Appl 1998, 27, 478.
14. Rose, L. J.; Channel, A. D.; Frye, C. J.; Capaccio, G. J Appl Polym Sci 1994, 54, 2119.
15. Clutton, E. Q.; Rose, L. J.; Capaccio, G. Plast Rubber Compos Process Appl 1998, 27, 478.
16. Laragon, J.; Dixon, N. M.; Gerrard, D. J.; Reed, W.; Kip, B. Macromolecules 1998, 31, 5845.
17. Gent, A. N.; Madan, S. J Polym Sci Part B: Polym Phys 1989, 27, 1529.
18. Kramer, E. J. Polym Eng Sci 1984, 24, 761.
19. Kramer, E. J.; Berger, L. L. Adv Polym Sci 1990, 91/92, 1.
20. Kausch, H.-H.; Plummer, C. J. G. Polymer 1994, 35, 3848.
21. G'Sell, C.; Jonas, J. J. J Mater Sci 1981, 16, 1956.
22. Gibson, A. G.; Jawad, S. A.; Davis, R. G.; Ward, I. M. Polymer 1982, 23, 349.
23. Ward, I. M. Mechanical Properties of Solid Polymers, 2nd ed.; Wiley-Interscience: New York, 1983; Chapter 4.
24. Peterlin, A. Colloid Polym Sci 1987, 265, 357.